Jia *et al. Blue Biotechnology* (2024) 1:7
https://doi.org/10.1186/s44315-024-00007-5

Blue Biotechnology

RESEARCH

Open Access

Characterization of salt brine sulfated polysaccharides: immunomodulatory activity based on gut microbiota

Xing Jia[1], Lin Ma[1], Meng Xiao[1], Dima Atehli[1], Yiheng Zhang[1], Yongshuai Liu[1], Wan Wang[1,2*], Changlu Wang[1] and Qingbin Guo[1*]

Abstract

A sulfated polysaccharide consisting of two components with molecular weights of 439 kDa and 16 kDa was extracted from the salt brine. The structural properties, immunomodulatory activity, in vitro fermentation behaviors, and effects of SP on regulating the gut microbiota were investigated. The chemical composition and monosaccharide composition analysis showed that the neutral sugar, protein, uronic acid, and sulfated group contents of SP were 60.42 ± 0.04%, 2.90 ± 0.01%, 13.34 ± 0.01% and 10.51 ± 0.01%, respectively, containing arabinose, galactose, glucose, rhamnose, xylose, mannose, and glucuronic acid in a molar ratio of 33.24:19.18:16.64:13.25:8.31:4.11:5.27. Results from the macrophage cell model showed that SP intervention improved the proliferation activity, phagocytosis of neutral red, and production of IL-6 and TNF-α in RAW 264.7. Furthermore, in vitro fermentation of SP by gut microbiota showed that SCFA production in all treatment groups was significantly higher than that of the blank control group after 48 h of fermentation, especially butyric acid which was 1.70 folds that of the control group. Moreover, long-term fermentation (48 h) of SP improved the diversity of microbiota, decreased the F/B ratio (30.75 at 0 h *vs.* 1.22 at 48 h), and promoted the growth of probiotics (*Parabacteroides*, *Bacteroidetes, Ruminococcaceae,* and *Phascolarctobacterium*). The positive regulatory effect of SP on the gut microbiota and its metabolites is considered a potential target for its immunomodulatory activity.

Keywords Brine, Sulfated polysaccharide, Structure, RAW 264.7 cells, In vitro fermentation

*Correspondence:
Wan Wang
wangwan@tust.edu.cn
Qingbin Guo
guoqingbin008322@tust.edu.cn
Full list of author information is available at the end of the article

Graphical abstract

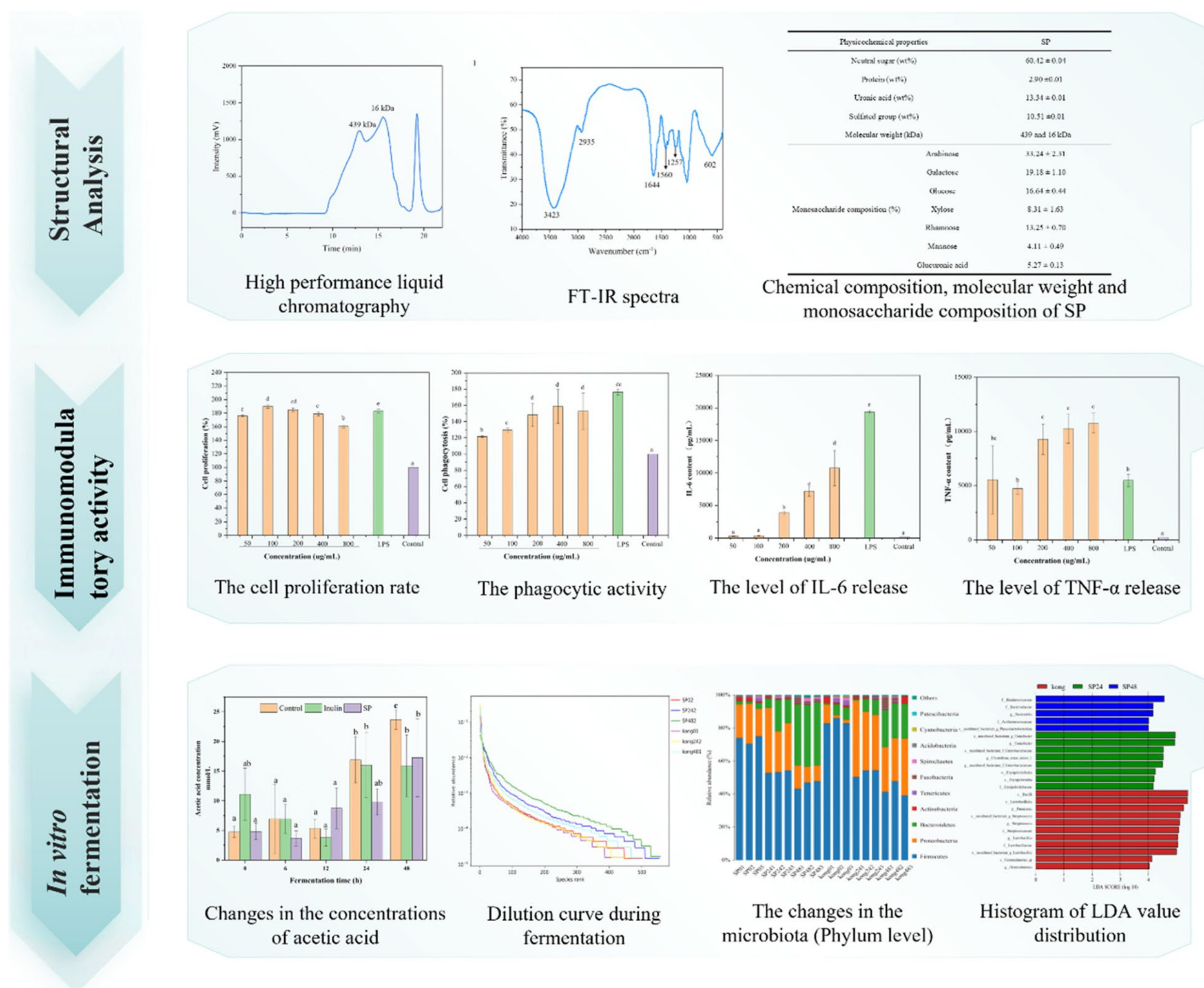

Introduction

Salt brine is the liquid that remains in salt ponds after seawater evaporates into salt by a combination of wind and sunlight [1]. Salt brine is rich in water-soluble and microbial-resistant sulfated polysaccharides, which mainly originate from marine organisms [2]. Sulfate groups can promote mutual recognition of polysaccharides with various substrates and cellular proteins. Meanwhile, the sulfate group replaces part of the hydroxyl groups of the polysaccharide, thus imparting various biological activities to the sulfated polysaccharide [3], such as probiotic, anticoagulant, antiviral, antioxidant, antitumor [4], and immunomodulatory activities [5, 6]. It has been reported that sulfated polysaccharides can exert immunomodulatory activity by regulating the signaling pathway in macrophages [7]. Kim et al. (2011) indicated that sulfated polysaccharides from *Enteromorpha prolifera* could stimulate the growth of macrophages and induce the mRNA expression and production of NO and various cytokines [8]. In addition, sulfated polysaccharides trigger an immune response in lymphocytes [6]. Sulfated polysaccharides can induce the proliferation of spleen lymphocytes, differentiate them into IgM-secreting plasma cells, and increase the expression of $CD71^+$, $CD25^+$, and mIg, thereby triggering the immune response of lymphocytes [9]. Liu et al. (2017) found that sulfated polysaccharide from *Porphyra haitanensis* significantly increased the secretion of TNF-α and IL-6, which play a key role in the acquired immune response by stimulating the production of antibodies and the development of effector T cells [10]. Furthermore, Sulfated polysaccharides can exert immunomodulatory activity by regulating natural killer cells to promote dendritic cell differentiation [3]. In brief, sulfated polysaccharides can exert immunomodulatory effects through various mechanisms.

In addition, non-starch polysaccharides cannot be degraded by digestive enzymes, while metabolized by gut microbiota [11], therefore sulfated polysaccharides can exert prebiotic activity by promoting the relative abundance of probiotics and regulating the gut microbiota [12]. Sulfated polysaccharides have been reported to increase the relative abundance of *Bacteroidetes* and decrease that of *Firmicutes*, thus promoting energy metabolism and ultimately reducing the obesity risk of the host [13]. Zhu et al. (2018) found that sulfated polysaccharides from sea cucumbers could increase the diversity of probiotics and inhibit the pathogenic bacteria [14]. Furthermore, sulfated polysaccharides can also exert prebiotic activity by being metabolized by the gut microbiota to produce beneficial metabolites such as short-chain fatty acids (SCFAs) including acetic acid, propionic acid, and butyric acid [15]. It has been confirmed that SCFAs can reduce the pH in the intestine to inhibit the proliferation of pathogens, thereby improving the intestinal epithelial cell barrier function [16]. Moreover, SCFAs have been shown to play an important role in alleviating obesity, chronic inflammation, and modulating immune responses [6, 17]. Therefore, the efficient and comprehensive utilization and functional evaluation of sulfation resources possess great value for the sustainable application of agricultural by-products and the development of nutritious and healthy foods. Although a large number of studies have reported that sulfated polysaccharides can regulate gut microbiota and have immunomodulatory activity, the interaction mechanism between the structural properties of salt brine sulfated polysaccharides, gut microbiota, and immune response is still unclear.

In this study, the structural properties of novel sulfated polysaccharides isolated from salt brine (SP) were investigated by a combination of chemical and spectroscopic methods including gas chromatography-mass spectrometry (GC–MS) and Fourier transform infrared spectrometer (FT-IR). In addition, the RAW 264.7 model was used to evaluate the immunomodulatory activity of SP. Furthermore, the regulatory effects of SP on the gut microbiota and SCFAs were studied using an in vitro fermentation test. This study aimed to develop novel sulfated polysaccharides that are high-value by-products of saltwater resources and provide a theoretical basis for clarifying the mechanism by which sulfated polysaccharides exert immune response functions based on the gut microbiota.

Materials and methods

Materials

Salt brine was provided by Tianjin Changlu Haijing Group Co., Ltd. (Tianjin, China) and was mainly from seawater in Bohai Bay, Tianjin. The salt brine was collected from April to June 2022 at a depth of approximately 1 m. Monosaccharide standards were purchased from Beijing Solarbio Science & Technology Co., Ltd. (Beijing, China). CCK-8 kit was purchased from Beijing Solaibao Technology Co., LTD. (Beijing, China). TNF-α ELISA kit and IL-6 ELISA kit were purchased from Hangzhou Lianke Biotechnology Co., LTD (Hangzhou, China). All other chemicals and reagents were of analytical grade unless specified otherwise.

Isolation of SP

Salt brine was filtered through 4 nm filter paper to remove impurities and then dialyzed using a dialysis bag (8000–14000 Da) with distilled water at room temperature for 2–3 d until the conductivity of the dialysate approached that of distilled water. The dialyzed sample was concentrated to one-third of its original volume and precipitated with ethanol (4 °C, 12 h) to a final concentration of 80% (v/v) ethanol in the system. The above solution was then centrifuged (4000 × g, 15 min, 4 °C) to obtain the precipitate, which was then freeze-dried to obtain SP.

Chemical composition analysis and molecular weight (Mw) determination

Neutral sugar content was determined using the phenol sulfuric acid method [18]. Protein content was determined using the bicinchoninic acid assay method [19]. The uronic acid content was determined using the m-hydroxyphenyl colorimetric method [20]. The sulfated group content was determined using the barium chloride gelatin method [21].

The Mw of SP was determined according to the method described by Xiao et al. (2024), with some modifications [22]. Briefly, the sample (2 mg) was dissolved in $NaNO_3$ solution (0.1 M, 1.0 mL) and filtered through a 0.2 μm polyethersulfone filter membrane to remove insoluble particles. The sample solution (20 μL) was then injected into the Shimadzu LC20 HPSEC system, which consisted of a Shimadzu RID-20 refractive index detector, a combination of HPSEC pump and Ultrahydrogel Linear Column (300 mm × 7.8 mm × 10 μm, Waters, Massachusetts, USA) used for determination of carbohydrates in the range of 10–1000 kDa. The different Mw of dextrans (10, 40, 70, 500, and 2000 kDa) were used as standards.

Monosaccharide composition analysis

The monosaccharide composition of SP was measured according to the method reported by Kang et al., (2023) with slight modifications [23]. The sample (10 mg) was dissolved with trifluoroacetic acid solution (3 M, 5 mL), and then hydrolyzed (120 ℃, 6 h). The hydrolysate was repeatedly evaporated with ethanol at 45 °C to remove excess hydrochloric acid and trifluoroacetic acid by a rotary evaporator. The above sample obtained by rotary evaporation was dissolved in ultrapure water (2 mL) and passed through a 0.22 μm polyethersulfone filter membrane. The Thermo ICS-5000 ion chromatography analysis system (Diane-ICS-5000$^+$, Thermo Fisher Scientific, Massachusetts, USA) is equipped with a pulse amperometer, Dionex CarboPacTM PA20 (3 mm × 150 mm) anion exchange column and a Dionex CarboPacTM PA20 (3 mm × 50 mm) protective column was used to determine monosaccharide composition of SP. The columns were maintained at 30 °C and performed gradient elution with ultrapure water, 0.2 M sodium hydroxide solution, and 0.1 M sodium acetate solution as the mobile phase. A quantitative monosaccharide standard solution was measured according to the above parameters to draw a standard curve.

FT-IR analysis

The sample (1 mg) and KBr (150 mg) were mixed and ground evenly, then pressed into pellets by compression machine (30 MPa, 30 s). The pressed pellets were scanned using a Fourier transform infrared spectrometer (Nicolet IS50, Thermo Fisher Scientific, Massachusetts, USA). The spectra were recorded at the absorbance mode from 4000 to 400 cm^{-1} at the resolution of 4 cm^{-1} and 32 scans were collected.

Immunomodulatory activity evaluation

Cell culture

RAW264.7 were cultured in RPMI-1640 medium (Gibco, Thermo Fisher Scientific, Massachusetts, USA) containing 10% fetal bovine serum (Gemini, Woodlandm, USA), 100 U/mL penicillin (Hyclone, Thermo Fisher Scientific, Massachusetts, USA), and 100 μg/mL streptomycin (Hyclone, Thermo Fisher Scientific, Massachusetts, USA), and incubated at 37 °C in a 5% CO_2 incubator. The cells were maintained at 37 °C in a 5% CO_2 incubator. RAW264.7 were divided into a control group (without SP intervention), positive control group (LPS: 1 μg/mL), and various concentrations of SP groups (50, 100, 200, 400, and 800 μg/mL).

Determination of cell proliferative activity

The effects of SP on the proliferative activity of RAW 264.7 were determined by the CCK-8 method. The RAW 264.7 of different groups were seeded and incubated in a 96-well flat-bottom plate at a cell density of 5×10^4 cells/well for 24 h, and the medium was discarded. Then, 100 μL of RPMI-1640 medium containing the control, LPS and SP sample was added, and the cells were incubated for 24 h. After discarding the medium, 10 μL of CCK-8 solution was added to each well and cultured at 37 °C, 5% CO_2, and 90% humidity for 4 h. The absorbance of the sample was measured at a wavelength of 450 nm using an enzyme-labeled instrument (Infinite 200 Pro, Männedorf, Tecan).

Determination of phagocytic activity

The RAW 264.7 of different groups were seeded and incubated in a 96-well flat-bottom plate with a cell density of 5×10^4 cells/well for 24 h, and the medium was discarded. Then, 100 μL of RPMI-1640 medium containing the control, LPS and SP sample was added, and the cells were incubated for 24 h. After the medium was discarded, 100 μL neutral red solution (0.1%) was added to each well and cultured at 37 °C, 5% CO_2, and 90% humidity for 2 h. Then, the cells were washed with PBS, cleaved with 200 μL cell lysate for 10 min, and the absorbance was determined at a wavelength of 540 nm using an enzyme-labeled instrument (Infinite 200 Pro, Männedorf, Tecan).

Determination of cytokines

The RAW 264.7 of different groups were seeded and incubated in a 24-well flat-bottom plate with a cell density of 1×10^5 cells/well for 24 h, and the medium was discarded. Then, 100 μL of RPMI-1640 medium containing the control, LPS and SP sample was added, and the cells were incubated for 24 h. The culture supernatant was collected to evaluate the production of TNF-α and IL-6 using ELISA kits (Hangzhou Lianke Biotechnology Co., LTD, Hangzhou, China).

In vitro fermentation properties of SP

The pig feces were collected from the colons of monoline Landrace pigs (Tianjin Guanghua Meat Co., Ltd.) fed a diet primarily consisting of corn bran, bean pulp, and buckwheat as fibre sources. The pigs were about 7 months old (approximately 120 kg). The collected feces were kept under an anaerobic condition and stored at -80 ℃.

SP was homogeneously dispersed into the fermentation medium to generate 1% (w/v) solution and mixed with pig feces (10%, w/v), then sealed and cultured in an anaerobic bag at 37 °C with shaking. One mL of fermentation sample was taken out at 0, 6, 12, 24 and 48 h, respectively, and centrifuged at 11,000 g for 20 min to collect the supernatant for pH and SCFAs determination. The specific determination methods are shown in 2.7.1 and 2.7.2. Porcine colon contents were added directly to anaerobic medium for fermentation as a control group.

Determination of pH

The pH of the fermentation supernatant at 0, 6, 12, 24, and 48 h was measured using a pH meter (PB-10; Sartorius, Gottingen, Germany).

Determination of SCFAs

The SCFA levels were determined using a GC-FID system equipped with a Nukol TM Fused Silica Capillary Column (60 mm × 0.25 mm × 0.25 μm) (Bruker 450 GC, Billerica, Massachusetts, USA). The chromatographic conditions were as follows: injector temperature, 200 °C; detector temperature, 250 °C; H_2 flow rate, 40 mL/min; and air flow rate, 400 mL/min. A standard curve of volatile free fatty acids was used to quantify SCFAs, with 2-ethylbutyrate as an internal standard.

16S rDNA analysis

Construction of MiSeq libraries and sequencing of 16S rDNA were performed according to the method reported by Wang et al. (2022) [24]. Total DNA was extracted from fermented colon contents, and its quantity was determined using a DNA isolation kit (Thermo Fisher Scientific, Waltham, MA, USA) and a UV spectrophotometer. PCR amplification of the V3-V4 region of the 16S rRNA gene was performed using primers 338F (5′-ACTCCTACGGGAGGCAGCA-3′) and 806R (5′-GGACTACHVGGGTWTCTAAT-3′). Illumina library preparation was performed according to the 16S Metagenomic Sequencing Library Preparation and sequenced on an Illumina® MiSeq (PE300) platform (Illumina, San Diego, CA, USA). Sequence data were analyzed using QIME version 1.8.0. Species annotation was performed for each operational taxonomic unit to obtain corresponding species information and abundance distribution. The taxon abundance of samples was analyzed and compared by Metastases at the phylum and genus classification levels. The structural differences between species were analyzed using α-diversity and the Shannon index.

Statistical analysis

The data are expressed as the mean ± standard deviation of three independent replicates. One-way analysis of variance (ANOVA) was performed using SPSS software (SPSS 25.0). $p < 0.05$ indicated a significant difference with Duncan's test.

Results and discussion

Physicochemical properties of SP

The chemical composition of SP is shown in Table 1. The neutral sugar, protein, uronic acid, and sulfate group content were 60.42 ± 0.04%, 2.90 ± 0.01%, 13.34 ± 0.01% and 10.51 ± 0.01%, respectively, indicating that SP is a sulfated polysaccharide with a small amount of protein, which was similar to the results of the chemical composition of marine polysaccharides reported by Wan et al. (2023) [25]. Nunes et al. (2019) reported that the carbohydrate content of SP extracted from salt brine in Aveiro on the North Coast of Portugal (Atlantic Ocean) in September and October were 39.6 ± 1.8% and 45.0 ± 3.3%, respectively [2]. Compared to the above results, a higher neutral sugar content was observed in the present study, which might be due to differences in area and season [3]. More specifically, the seaweed grows in large quantities in June and July; therefore, the total sugar content of SP extracted in June was higher. The molecular weight distribution of SP is shown in Fig. 1A. Two main peaks were observed in the liquid chromatogram, indicating that SP was composed of two components with Mw of 439 kDa and 16 kDa.

Monosaccharide composition analysis

The monosaccharide composition of SP was measured by an ion chromatography analysis system, and the results are shown in Table 1. The monosaccharides of SP were mainly composed of arabinose, galactose, glucose, rhamnose, xylose, mannose, and glucuronic acid in a molar ratio of 33.24:19.18:16.64:13.25:8.31:4.11:5.27. In contrast, the monosaccharides of SP extracted from salt brine in Aveiro by Nunes et al. (2019) were mainly composed of arabinose (2–11%), galactose (10–17%), glucose (8–15%), fucose (11–17%), rhamnose (5–8%), xylose

Table 1 Chemical composition, molecular weight and monosaccharide composition of SP

Physicochemical properties		SP
Neutral sugar (wt%)		60.42 ± 0.04
Protein (wt%)		2.90 ± 0.01
Uronic acid (wt%)		13.34 ± 0.01
Sulfated group (wt%)		10.51 ± 0.01
Molecular weight (kDa)		439 and 16
Monosaccharide composition (%)	Arabinose	33.24 ± 2.31
	Galactose	19.18 ± 1.10
	Glucose	16.64 ± 0.44
	Xylose	8.31 ± 1.63
	Rhamnose	13.25 ± 0.70
	Mannose	4.11 ± 0.49
	Glucuronic acid	5.27 ± 0.13

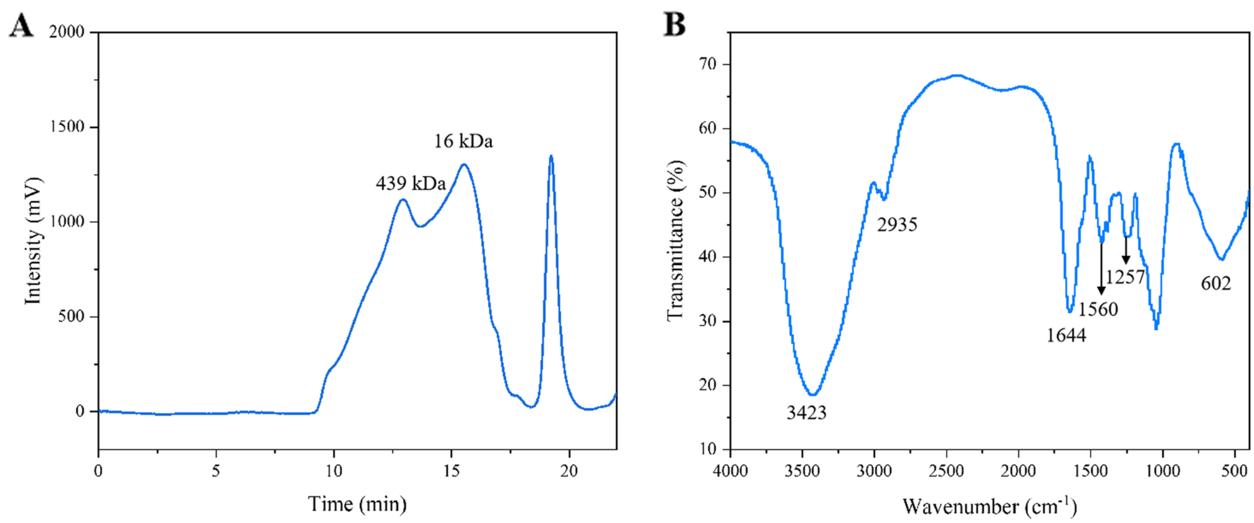

Fig. 1 HPSEC profile (**A**) and FT-IR spectra (**B**) of SP

(4–11%), and mannose (4–11%) [2]. This is because SP is mainly derived from the extracellular polysaccharides of seaweed or microalgae; therefore, the differences in and relative molar ratios of monosaccharides are due to species differences and genotypes caused by the geographical isolation of marine organisms [2].

FT-IR spectrometric analysis

The FT-IR spectrum of SP is shown in Fig. 1B. It could be observed that a wide and strong absorption peak at 3423 cm^{-1} caused by the O–H stretching vibration of intermolecular and intermolecular hydrogen bonds [12], and the peak at 2935 cm^{-1} caused by the C-H stretching vibration of the CH_3 group [14], which are the characteristic structure of polysaccharides. In addition, the absorption peak at 1644 cm^{-1} represents the stretching vibration of the C=O group on the acetyl or carboxyl group, indicating the presence of uronic acid [26]. The absorption peak at 1560 cm^{-1} was the characteristic absorption peak of -CONH-, indicating the presence of the protein [21]. The characteristic absorption peaks of uronic acid and protein were consistent with the chemical composition of SP (Table 1). Furthermore, the stretching vibrations at 1257 cm^{-1} and 602 cm^{-1} demonstrated the presence of S=O [27], which once again confirmed that SP is a sulfated polysaccharide.

Immunomodulatory activity of SP

Effect of SP on proliferative activity of RAW264.7

RAW264.7 has phagocytosis and satiation, and is considered to be an ideal in vitro model to investigate the immune response ability of macrophages [28]. The cytotoxic effects of SP at gradient concentrations (50, 100, 200, 400, and 800 μg/mL) on RAW264.7 cells were detected using the CCK-8 method, and the results are shown in Fig. 2A. The results showed that SP not only had no cytotoxicity to RAW264.7 but promoted cell proliferation in the experimental concentration range of 50–800 μg/mL compared with the control group. The cell proliferation rate reached a maximum of 189.95% at the SP concentration of 400 μg/mL, indicating that SP can significantly promote the proliferation of RAW264.7 cells ($p < 0.05$). This result was consistent with that reported by Peng et al. (2024) [29]. They investigated the proliferative effect of *Armeniaca Sibirica* L. polysaccharides (AP-1) on RAW264.7 cells. The results showed that AP-1 was not toxic to RAW264.7 cells in the concentration range of 50–1000 μg/mL. The effect of AP-1 on cell viability was high at low dose concentrations (50 μg/mL-100 μg/mL) and decreased at high dose concentrations (100 μg/mL-1000 μg/mL).

Effect of SP on phagocytosis of RAW 264.7 cells

Phagocytosis is one of the basic functions of macrophages and, to some extent, reflects the state of immune function. Macrophages can remove damaged cells and pathogens via phagocytosis to maintain homeostasis in the body [30]. The effect of SP with different concentrations (50–800 μg/mL) on phagocytosis of RAW 264.7 cells was evaluated by the neutral red method, and the results are shown in Fig. 2B. Compared with the control group, SP could significantly increase the phagocytosis of RAW264.7 cells ($p < 0.05$). In particular, the phagocytosis of RAW264.7 cells reached 129.58 ± 0.14% intervented by SP at a concentration of 100 μg/mL, which was significantly higher than that of LPS intervention. This result is

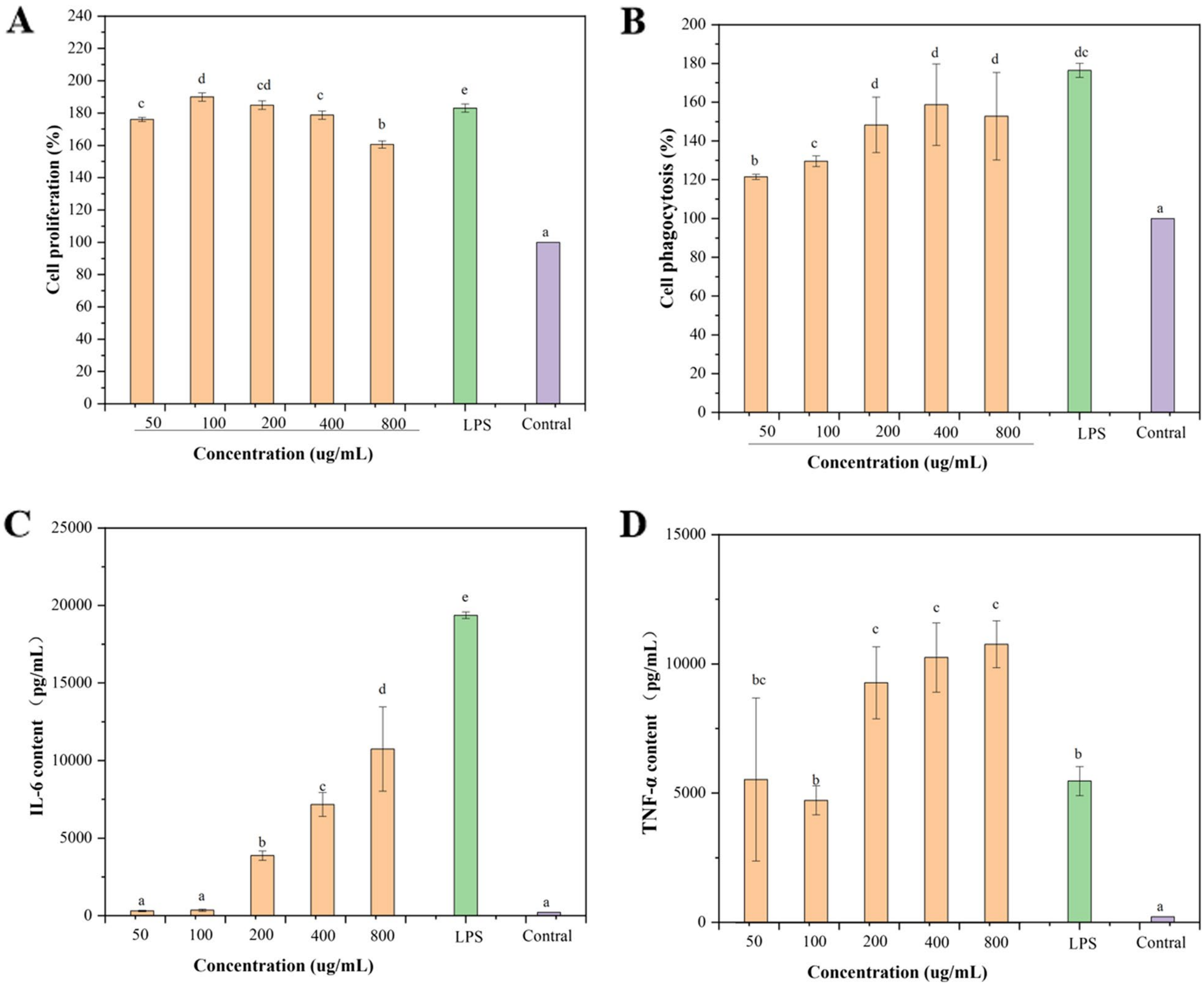

Fig. 2 Effects of SP on proliferation (**A**), phagocytosis (**B**), IL-6 (**C**) and TNF-α (**D**) release from RAW 264.7. Different lowercase letters on the bars represent significant differences between the data ($p < 0.05$)

consistent with that reported by Li et al. (2024), that the polysaccharides isolated from *Dioscotea opposita* could increase the cell viability of RAW 264.7 cells in low concentration intervention, then decreased with the polysaccharide concentrations increased [31]. In addition, it has been reported that sulfated polysaccharides from *Ganoderma lucidum* can enhance the phagocytic ability of macrophages more than neutral polysaccharides, which confirmed that the phagocytic activity of sulfated polysaccharides is not only affected by the concentration but also by the degree of sulfated group substitution [32].

Effects of SP on cytokine release

IL-6 is secreted by macrophages and participates in many physiological processes such as immune regulation, inflammatory response and homeostasis regulation [3]. The effect of SP on IL-6 release from RAW 264.7 cells is shown in Fig. 2C. Compared with the control group, the concentration of IL-6 significantly increased from 310.33 ± 39 pg/mL to 10,750.67 ± 2708 pg/mL with the SP concentration increased from 50 μg/mL to 800 μg/mL ($p < 0.05$), indicating that SP induced IL-6 release from RAW 264.7 cells in a dose-dependent manner. This is consistent with the results of Bi et al. (2024) that the novel polysaccharide CVPW-1 isolated from *Coriolus versicolor* promoted the release of IL-6 from RAW 264.7 in a dose-dependent manner (0–500 μg/mL) [33]. Differently, compared with present results, the effect of CVPW-1 intervention in promoting IL-6 release was lower than that of SP at the same concentration, which may be due to the higher sulfate group content of SP (10.51 ± 0.01%) than that of CVPW-1 (n.d.). Similarly, Liu et al. (2017) reported that the polysaccharide of

Porphyra haitanensis, which had a high sulfate group content (14.67%), could significantly increase IL-6 levels in the serum of healthy mice [10].

TNF-α is an inflammatory cytokine that is primarily secreted by macrophages. It participates in cell signal transduction, immune regulation and tumor cell apoptosis by binding to specific receptors on the tumor cell membrane [30]. The effect of SP concentration on TNF-α release from macrophages is shown in Fig. 2D. The TNF-α concentration in the cell supernatant increased from 5526.56 ± 3153 pg/mL to 10,763.22 ± 908 pg/mL with the SP concentration increased from 50 μg/mL to 800 μg/mL, indicating that SP intervention could effectively activate macrophages to release TNF-α in a dose-dependent manner. Similarly, the polysaccharide FCF-2 purified from *Cucumaria frondosa* by Stefaniak-Vidarsson et al. (2017) could also stimulate macrophages to secrete TNF-α [7]. The TNF-α levels in the supernatant of 100 μg/mL FCF-2 intervention was 1581 ± 61 pg/mL, which was lower than the TNF-α released after the intervention of the same concentration of SP in this study, which might be due to the higher uronic acid content (13.34%) and sulfated group content (10.51%) of SP.

In summary, SP significantly enhanced cell viability, phagocytosis, and cytokine release in RAW 264.7, which may be due to the negative charge attached to the sulfated group, thereby enhancing the interaction with cationic protein receptors on the cell membrane surface. For example, SPs bind to the toll-like receptor on the surface of T lymphocytes, and the receptor forms a complex with the adaptor protein MyD88 to activate signal transduction pathways, such as the MAPK/NF-κB signaling pathways, to mediate the release of inflammatory cytokines [3]. In addition, the mannose receptor is an important pattern recognition and endocytic receptor in the innate immune system, which is mainly expressed by macrophages and can recognize mannose, fucose, and acetyl glucosamine [6]. SPs containing mannose promote phagocytosis of macrophages and participate in the innate immune response by interacting with mannose receptors [34]. Furthermore, CD14 is a receptor with a high affinity for sulfated polysaccharides and is a marker for determining macrophage differentiation. The binding of sulfated polysaccharides to CD14 can activate the signal transduction cascade, thereby stimulating the immune activity of macrophages [35]. Thus, the sulfated group content of polysaccharides is one of the key factors in their immunomodulatory effects. Similarly, Leiro, et al. reported that the immunological activity of Ulva rigida *C. Agardh* polysaccharides was reduced after removal of the sulfated group [36]. Therefore, the structure–activity relationship between the molecular structure (the sulfated group content, Mw, etc.) and the immunomodulatory activity of SP will be further verified in our subsequent studies.

In vitro fermentation

Changes in pH during fermentation

Carbohydrates are degraded by gut microbiota during colonic fermentation to produce organic acids; therefore, pH can reflect the utilization of carbohydrates [24]. The pH changes in the fermentation supernatant during SP fermentation are shown in Fig. 3A. The pH of the fermentation broth in both the control and SP groups showed a trend of first decreased significantly and then increased slightly. This result was consistent with the trend reported by Cui et al. (2021), in which the pH of the fermentation broth of laminarin-type polysaccharide purified from *Sargassum henslowianum* decreased within 12 h and increased at the end of fermentation [21]. This may be due to the preferential utilization of carbon sources and SP in the colonic contents by the gut microbiota to produce organic acids (pH decreases), followed by the depletion of carbon sources, and the utilization of lactic acid and organic nitrogen sources to release amino nitrogen, resulting in a slight increase in pH [17]. However, the lowest pH values in the control and SP groups were at 12 h (6.46 ± 0.38) and 24 h (6.60 ± 0.30), respectively. The reason for this difference is that SP, as an additional dietary fiber, took longer to be utilized by the gut microbiota, thus delaying the decrease in the pH of the fermentation broth. The results showed that SP fermentation could reduce the pH value of colon contents, which was not only beneficial for inhibiting pathogenic bacteria, but also the short-chain fatty acids produced could participate in the signal transduction of intestinal epithelial cells and enhance the intestinal barrier function [15, 37].

Changes in SCFAs

Carbohydrates are metabolized by gut microbiota to produce SCFAs, which play an indispensable role in maintaining host physiological activities and cellular energy homeostasis [38]. Changes in SCFAs content during fermentation are generally considered a crucial indicator of the fermentation properties of polysaccharides [39]. The content of SCFAs (acetic acid, propionic acid, and butyric acid) at different fermentation times is shown in Fig. 3 (B-D). The concentrations of acetic acid, propionic acid, and butyric acid in the SP group increased with fermentation time, especially reaching 18.93 ± 5.23 mmol/L, 6.07 ± 0.68 mmol/L, and 3.38 ± 0.38 mmol/L at 48 h of fermentation, which were 1.21-, 1.62 and 1.70 folds that of the control group, respectively. Acetate may induce the immune response of the host against pathogenic bacteria and regulate the balance of gut microbiota [40]. In

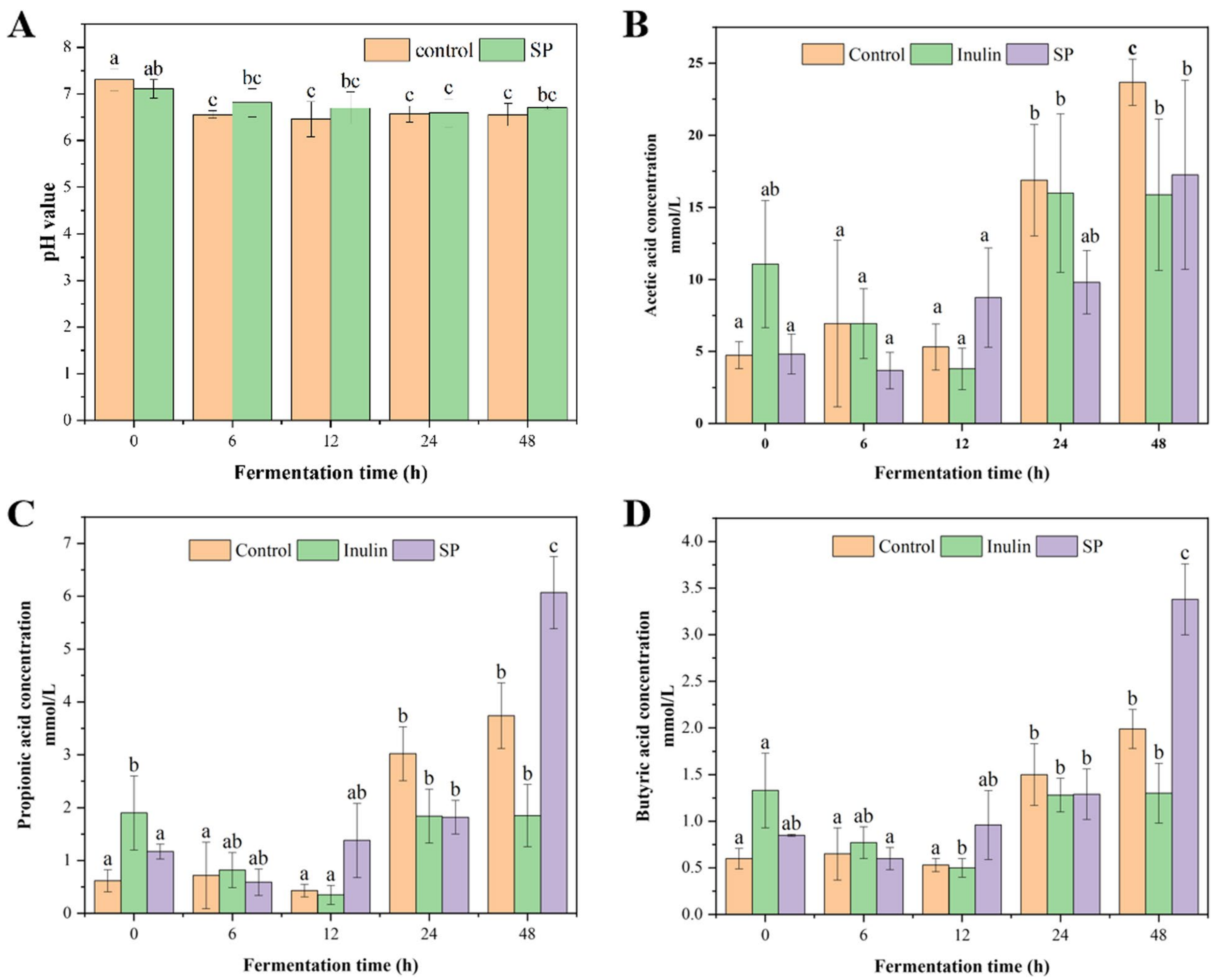

Fig. 3 Changes in pH (**A**) and concentrations of acetic acid (**B**), propionic acid (**C**) and butyric acid (**D**) in fermentation solution Different lowercase letters on the bars represent significant differences between the data ($p < 0.05$)

addition, propionate supplementation has been reported to increase Treg immune cells, suggesting the possibility of propionate as an immunomodulator for adjuvant therapy in autoimmune diseases [41]. Butyrate is the main energy source for intestinal epithelial cells and plays an important role in regulating intestinal barrier function, immune cell proliferation, and the intestinal immune response [42]. The results showed that SP could be utilized by the gut microbiota to produce SCFAs, especially butyric acid, suggesting that butyric acid may be the link between SP and its immunomodulatory activity.

α-diversity analysis

The results of SCFAs showed that the metabolites produced by the utilization of SP increased rapidly at 24–48 h, the gut microbiota of the SP group was speculated to have changed significantly during this period. Therefore, the colon contents of samples fermented for 0 h (SP0), 24 h (SP24) and 48 h (SP48) were subjected to 16S rDNA analysis, and the results of α-diversity: dilution curve, Shannon curve and rank abundance curve are shown in Fig. 4 (A-C). α-Diversity generally reflects the richness of the microbiota within a group [43]. As shown in Fig. 4 (A-C), the curves of all groups eventually flattened as the number of sequences sampled increased, indicating that the species diversity in the colon content samples was high enough for subsequent analysis [44]. In addition, it could be observed that there was no significant difference in the number of OTUs (dilution curve) and Shannon index (Shannon curve) in the control group with the fermentation time, while the SP group showed a significant up-regulation, indicating that SP intervention can improve species diversity of colon contents in a time-dependent manner. Furthermore, the rank abundance curve in Fig. 4C could also reflect the richness and uniformity of the gut microbiota. The rank

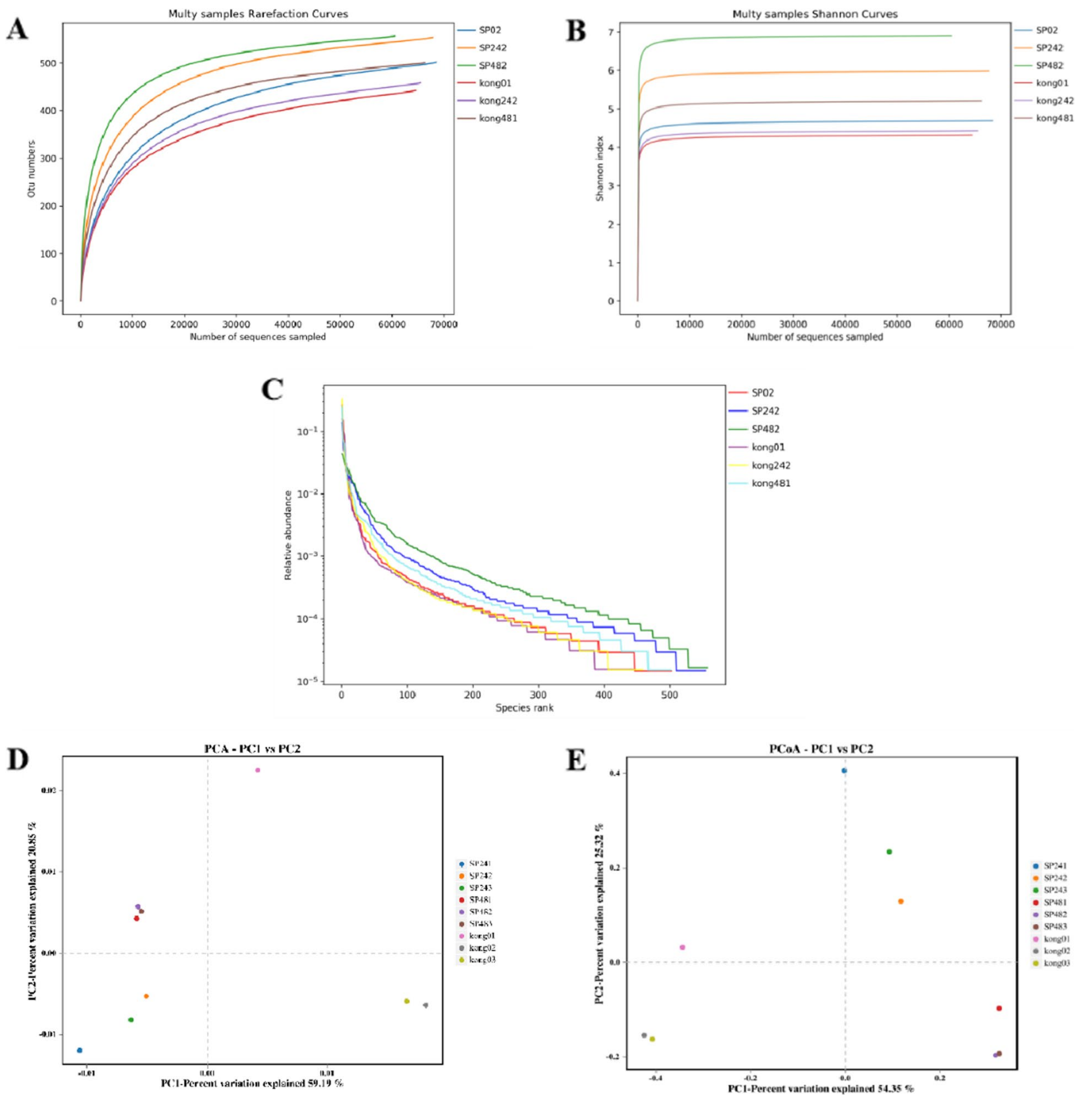

Fig. 4 Dilution curve (**A**), shannon curve (**B**), rank abundance curve (**C**), Principal component analysis (**D**) and principal coordinate analysis (**E**) of gut microbiota. The SP0, SP24, and SP48 represent colonic content microbiota samples at 0 h, 24 h, and 48 h of SP fermentation, respectively. The kong0, kong24, and kong48 represent the colon content microbiota samples at 0 h, 24 h, and 48 h of blank fermentation (without SP), respectively

abundance curve of the SP group was wider and flatter than that of the blank control group, indicating that the richness and uniformity of species composition in the SP group improved [45].

PCA and PCoA analysis in the fermentation process

Principal component analysis (PCA) and principal coordinate analysis (PCoA) are dimensionality reduction sequencing methods that reflect similarities and differences in the composition of the gut microbiota between samples. The closer the projections on the axis between the samples, the smaller the difference in microbiota composition, and vice versa [46]. In this study, PCA and PCoA analyses based on the Bray–Curtis algorithm were used to analyze the similarities and differences in the gut microbiota between the blank control and SP groups at

24 and 48 h of fermentation, as shown in Fig. 4 D-E. It could be observed that the close distance between different samples in the same group indicated that the data within the group has good repeatability, and the discreteness between samples in different groups indicated that SP fermentation could significantly change the composition of gut microbiota. Meanwhile, the discreteness between the SP groups and the blank control group increased with the extension of fermentation time, whether in PCA or PCoA analysis, which once again confirmed that the composition of the gut microbiota changed significantly with the increase in SP fermentation time.

Analysis of gut microbiota at the phylum level

To further investigate the effect of SP on gut microbiota, the composition of the gut microbiota was analyzed at the phylum level, as shown in Fig. 5A. SP intervention increased the relative abundance of Bacteroidetes and reduced the relative abundance of Firmicutes compared to the blank control group at the corresponding time. Moreover, with the increase of SP fermentation time from 0 to 24 h, the relative abundance of Firmicutes decreased from 73.18% to 46.04%, the relative abundance of Bacteroidetes increased from 2.38% to 37.64%, and the ratio of Firmicutes to Bacteroidetes (F/B ratio) decreased from 30.75 to 1.22. This might be because Bacteroidetes had more polysaccharide hydrolases and carbohydrate metabolism pathways to metabolize polysaccharides to produce SCFAs than Firmicutes, which also explained why SP intervention could increase the concentration of SCFAs in colon contents [37]. In addition, it is reported that the F/B ratio in the gut microbiota is positively correlated with obesity [47], indicating that SP has the potential to promote energy metabolism and alleviate obesity and diabetes by regulating the gut microbiota. Furthermore, the relative abundance of Proteobacteria decreased significantly under the intervention

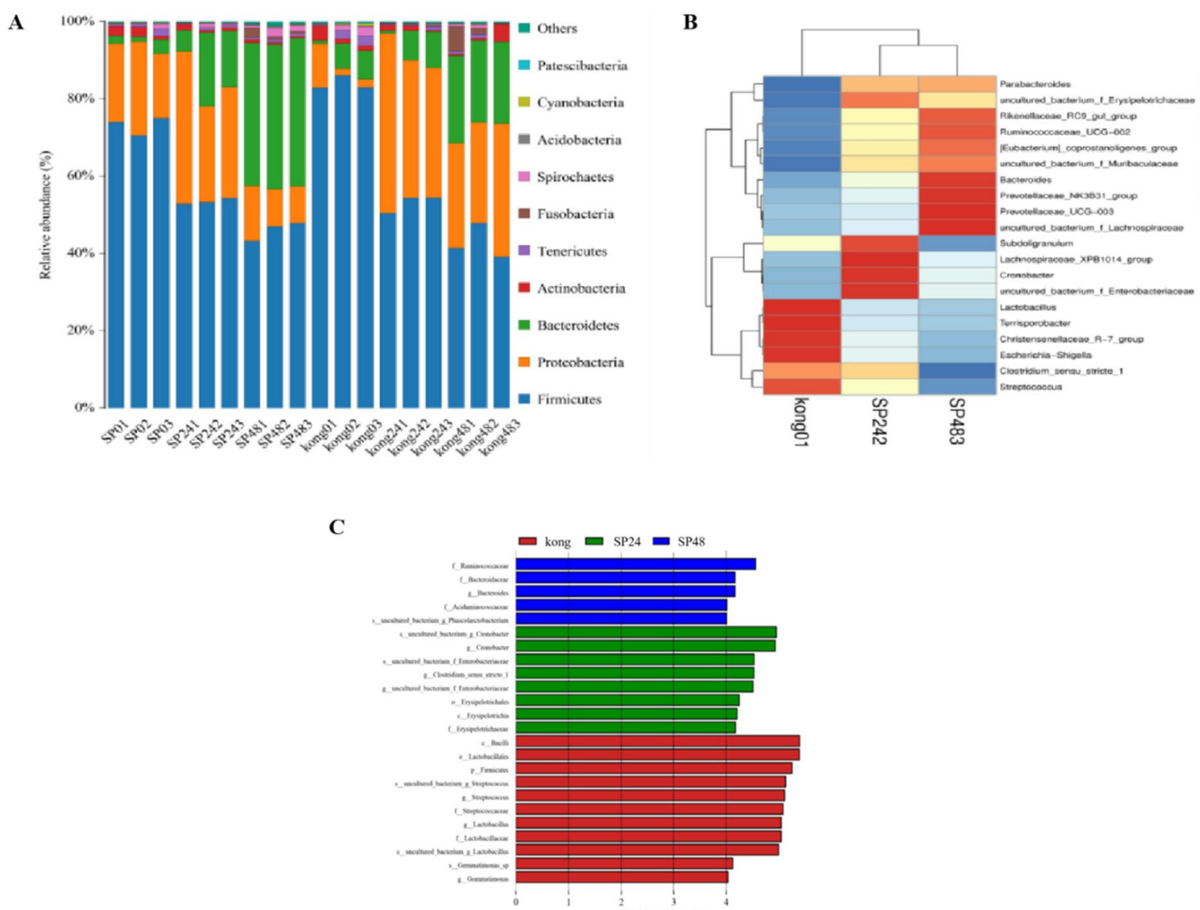

Fig. 5 The microbiota composition (**A**), Heat map analysis (**B**) and Histogram of LDA value distribution (**C**) of SP after in vitro fermentation for 0, 24 and 48 h (Phylum level) The SP0, SP24, and SP48 represent colonic content microbiota samples at 0 h, 24 h, and 48 h of SP fermentation, respectively. The kong0, kong24, and kong48 represent the colon content microbiota samples at 0 h, 24 h, and 48 h of blank fermentation (without SP), respectively

of SP in a time-dependent manner, which meant that SP had the potential to inhibit the proliferation of pathogenic bacteria, since almost all Proteobacteria were opportunistic pathogens (e.g., Escherichia-Shigella and Enterobacteriaceae).

Heatmap analysis of gut microbiota at the genus level

The composition of gut microbiota was analyzed at the genus level, as shown in the heatmap (Fig. 5B), which could visually reflect the abundance difference in the microbiota composition between groups through color gradients and clusters according to the similarity of species abundance. It was observed that SP intervention significantly increased the relative abundances of *Parabacteroides*, *Bacteroidetes*, *Ruminococcaceae_UCG-002*, *Prevotellaceae_NK3B31_group*, and *Prevotellaceae_UCG-003* compared to the control group. Previous research has reported that *Prevotellaceae*, *Bacteroidetes* and *Ruminococcaceae* are all SCFAs producing bacteria that can maintain immune homeostasis by interacting with G protein-coupled receptors [48]. It has also been reported that *Parabacteroides* can play an immunomodulatory role in promoting macrophage polarization by activating G-protein-coupled bile acid receptors through the production of specific secondary bile acids [49]. In addition, the relative abundance of *Coprostanoligenes* increased from 0.11% to 2.26% after SP fermentation. *Coprostanoligenes* can break down cholesterol into non-absorbable coprosterols, which are excreted in feces, indicating that SP supplementation can effectively relieve hyperlipidemia [42]. In addition, the relative abundance of *Terrisporobacter*, *Escherichia-Shigella*, *Streptococcus,* and *Helicobacter* significantly decreased compared to that in the control group. *Streptococcus* is a conditional pathogen that can cause purulent inflammation and hypersensitivity [17]. Excessive abundance of *Escherich-Shigella* can lead to the loss of intestinal immune barrier function, causing gastrointestinal infection and diarrhea syndrome [50]. *Helicobacter* can activate inflammasomes, inducing host inflammation and immune system imbalances. In addition, SP intervention significantly decreased the relative abundance of *Christensenellaceae* and *Clostridium* (belonging to Firmicutes), which was consistent with the trend in species composition at the phylum level. The results showed that SP intervention could inhibit the relative abundance of conditional pathogens and promote the growth of probiotics, which is of great significance for positively regulating the homeostasis of gut microbiota and intestinal immune function.

LEfSe analysis

LEfSe analysis can be used to explore phenotypic biomarkers that have a significant impact on differences in microbial species between groups [45]. The phenotypic biomarkers with LDA > 4 and $p < 0.05$ in the gut microbiota of different groups are presented in Fig. 5C. Eleven microorganisms were dominant in the control group, especially p_*Firmicutes,* including c_*Bacilli*, o *Lactobacillales*, and g_*Streptococcus, which* had the most significant differences. However, the SP intervention groups showed significantly different differential biomarkers; that is, g_*Cronobacter* and o_*Enterobacteriaceae* were dominant in the SP24 group, and f_*Ruminococcaceae*, f_*Bacteroidaceae*, g_*Bacteroides*, f_*Acidaminococcaceae*, and g_*Phascolarctobacterium* were dominant in the SP48 group. It has been reported that succinate, a product of *Bacteroides* and *Parabacteroides*, could serve as a growth substrate for *Phascolarctobacterium* and jointly promote lipid metabolism [51], confirming the potential of SP to regulate energy metabolism disorders. In addition, *Ruminococcaceae* has been reported to metabolize and produce glucomannan polysaccharides, which can activate the immune system to produce the cytokine TNF-α [51]. The results of the study confirmed that although SP intervention may temporarily cause the growth of conditional pathogens in the early stage of fermentation (0–24 h), from a long-term perspective (24–48 h), SP intervention can reshape the gut microbiota and has the potential to regulate immune response and lipid metabolism.

Conclusion

A sulfated polysaccharide (SP) consisting of two components with molecular weights of 439 kDa and 16 kDa was isolated from salt brine and characterized for its structural properties, immunomodulatory activity, in vitro fermentation behaviors, and effects on the regulation of gut microbiota. SP is rich in sulfate groups and is composed of arabinose, galactose, glucose, rhamnose, xylose, mannose and glucuronic acid in the molar ratio of 33.24:19.18:16.64:13.25:8.31:4.11:5.27. In addition, SP exhibited a significant immunomodulatory effect on macrophages in proliferation activity, phagocytosis of neutral red, and production of cytokines, which is related to its higher level of sulfate groups. Meanwhile, long-term fermentation (48 h) of SP could positively regulate the gut microbiota (improve bacterial diversity, decrease the F/B ratio, and promote the growth of probiotics) and be metabolized to produce SCFAs (especially butyric acid), which are considered targets of its immunomodulatory activity. The knowledge obtained in this study can provide a theoretical basis for the high-value utilization of saltwater and the development of SP, and promote its future application in functional foods.

Abbreviations

SP	Sulfated polysaccharide
SCFAs	Short-chain fatty acids

GC-MS	Gas chromatography-mass spectrometry
FT-IR	Fourier transform infrared spectrometer
Mw	Molecular weight
ANOVA	One-way analysis of variance
AP-1	*Armeniaca Sibirica* L. polysaccharides
PCA	Principal component analysis
PCoA	Principal coordinate analysis

Acknowledgements
Not applicable.

Authors' contributions
X. J.: Writing – original draft, Investigation, Formal analysis, Data curation. L. M.: Writing – original draft, Data curation. M. X.: Investigation, Formal analysis, Data curation. Dima Atehlia: Supervision, Investigation. Y. H. Z. and Y. S. L.: Methodology, Visualization, Investigation. W. W.: Writing – review & editing, Formal analysis. C. L. W.: Methodology, Formal analysis, Data curation. Q. B. G.: Writing –review & editing, Project administration, Funding acquisition, Formal analysis.

Funding
This work was supported by the "National Natural Science Foundation of China" (No. 32272270, 32072173), the Project of Tianjin Science and Technology Program (21ZYJDJC00110), the Open Project Program of the State Key Laboratory of Food Nutrition and Safety, Tianjin University of Science & Technology (Grant No. SKLFNS-KF-202103, SKLFNS-KF-202004), and Tianjin Research Innovation Project for Postgraduate Students (2022BKY129).

Availability of data and materials
No datasets were generated or analysed during the current study.

Declarations

Ethics approval and consent to participate
Not applicable.

Consent for publication
Not applicable.

Competing interests
The authors declare no competing interests.

Author details
[1]State Key Laboratory of Food Nutrition and Safety, Tianjin University of Science and Technology, No. 29, 13th Avenue, TEDA, Tianjin 300457, China. [2]College of Food Science and Engineering, Tianjin University of Science and Technology, No. 29, 13Th Avenue, TEDA, Tianjin 300457, China.

Received: 30 May 2024 Accepted: 8 July 2024
Published online: 17 September 2024

References

1. Bryan CR, Knight AW, Katona RM, Sanchez AC, Schindelholz EJ, Schaller RF. Physical and chemical properties of sea salt deliquescent brines as a function of temperature and relative humidity. Sci Total Environ. 2022;824:154462. https://doi.org/10.1016/j.scitotenv.2022.154462.
2. Nunes C, Rocha A, Quitério P, Ferreira SS, Correia A, Vilanova M, Coimbra MA. Salt pan brine water as a sustainable source of sulphated polysaccharides with immunostimulatory activity. Int J Biol Macromol. 2019;133:235–42. https://doi.org/10.1016/j.ijbiomac.2019.04.021.
3. Kang J, Jia X, Wang N, Xiao M, Song S, Wu S, Li Z, Wang S, Cui SW, Guo Q. Insights into the structure-bioactivity relationships of marine sulfated polysaccharides: A review. Food Hydrocoll. 2022;123:107049. https://doi.org/10.1016/j.foodhyd.2021.107049.
4. Gupta S, Abu-Ghannam N. Bioactive potential and possible health effects of edible brown seaweeds. Trends Food Sci Technol. 2011;22:315–26. https://doi.org/10.1016/j.tifs.2011.03.011.
5. Rudtanatip T, Lynch SA, Wongprasert K, Culloty SC. Assessment of the effects of sulfated polysaccharides extracted from the red seaweed Irish moss Chondrus crispus on the immune-stimulant activity in mussels Mytilus spp. Fish Shellfish Immunol. 2018;75:284–90. https://doi.org/10.1016/j.fsi.2018.02.014.
6. Huang L, Shen M, Morris GA, Xie J. Sulfated polysaccharides: Immunomodulation and signaling mechanisms. Trends Food Sci Technol. 2019;92:1–11. https://doi.org/10.1016/j.tifs.2019.08.008.
7. Stefaniak-Vidarsson MM, Kale VA, Gudjónsdóttir M, Marteinsdottir G, Fridjonsson O, Hreggvidsson GO, Sigurjonsson OE, Omarsdottir S, Kristbergsson K. Bioactive effect of sulphated polysaccharides derived from orange-footed sea cucumber (Cucumaria frondosa) toward THP-1 macrophages. Bioact Carbohydr Diet Fibre. 2017;12:14–9. https://doi.org/10.1016/j.bcdf.2017.09.002.
8. Kim J-K, Cho ML, Karnjanapratum S, Shin I-S, You SG. In vitro and in vivo immunomodulatory activity of sulfated polysaccharides from Enteromorpha prolifera. Int J Biol Macromol. 2011;49:1051–8. https://doi.org/10.1016/j.ijbiomac.2011.08.032.
9. Zhang P, Liu W, Peng Y, Han B, Yang Y. Toll like receptor 4 (TLR4) mediates the stimulating activities of chitosan oligosaccharide on macrophages. Int Immunopharmacol. 2014;23:254–61. https://doi.org/10.1016/j.intimp.2014.09.007.
10. Liu Q, Xu S, Li L, Pan T, Shi C, Liu H, Cao M, Su W, Liu G. In vitro and in vivo immunomodulatory activity of sulfated polysaccharide from Porphyra haitanensis. Carbohydr Polym. 2017;165:189–96. https://doi.org/10.1016/j.carbpol.2017.02.032.
11. Barlow GM, Lin EA, Mathur R. An overview of the roles of the gut microbiome in obesity and diabetes. Nutr Ther Interv Diabetes Metab Syndr. 2018: 65–91. https://doi.org/10.1016/B978-0-12-812019-4.00006-4.
12. Ye Y, Ji D, You L, Zhou L, Zhao Z, Brennan C. Structural properties and protective effect of Sargassum fusiforme polysaccharides against ultraviolet B radiation in hairless Kun Ming mice. J Funct Foods. 2018;43:8–16. https://doi.org/10.1016/j.jff.2018.01.025.
13. Chen L, Xu W, Chen D, Chen G, Liu J, Zeng X, Shao R, Zhu H. Digestibility of sulfated polysaccharide from the brown seaweed Ascophyllum nodosum and its effect on the human gut microbiota in vitro. Int J Biol Macromol. 2018;112:1055–61. https://doi.org/10.1016/j.ijbiomac.2018.01.183.
14. Zhu Z, Zhu B, Sun Y, Ai C, Wu S, Wang L, Song S, Liu X. Sulfated polysaccharide from sea cucumber modulates the gut microbiota and its metabolites in normal mice. Int J Biol Macromol. 2018;120:502–12. https://doi.org/10.1016/j.ijbiomac.2018.08.098.
15. Wang W, Zhao X, Ma Y, Zhang J, Xu C, Ma J, Hussain MA, Hou J, Qian S. Alleviating effect of *Lacticaseibacillus rhamnosus* 1.0320 combined with dihydromyricetin on acute alcohol exposure-induced hepatic impairment: based on short-chain fatty acids and adenosine 5′-monophosphate-activated protein kinase-mediated lipid metabolism signaling pathway. J Agric Food Chem. 2023;71:4837–50. https://doi.org/10.1021/acs.jafc.2c08523.
16. Ai C, Duan M, Ma N, Sun X, Yang J, Wen C, Sun Y, Zhao N, Song S. Sulfated polysaccharides from pacific abalone reduce diet-induced obesity by modulating the gut microbiota. J Funct Foods. 2018;47:211–9. https://doi.org/10.1016/j.jff.2018.05.061.
17. Shang Q, Jiang H, Cai C, Hao J, Li G, Yu G. Gut microbiota fermentation of marine polysaccharides and its effects on intestinal ecology: An overview. Carbohydr Polym. 2018;179:173–85. https://doi.org/10.1016/j.carbpol.2017.09.059.
18. DuBois M, Gilles KA, Hamilton JK, Rebers PA, Smith F. Colorimetric method for determination of sugars and related substances. Anal Chem. 1956;28:350–6. https://doi.org/10.1021/ac60111a017.
19. Cortés-Ríos J, Zárate AM, Figueroa JD, Medina J, Fuentes-Lemus E, Rodríguez-Fernández M, Aliaga M, López-Alarcón C. Protein quantification by bicinchoninic acid (BCA) assay follows complex kinetics and can be performed at short incubation times. Anal Biochem. 2020;608:113904. https://doi.org/10.1016/j.ab.2020.113904.
20. Wang N, Wu Y, Jia G, Wang C, Xiao D, Goff HD, Guo Q. Structural characterization and immunomodulatory activity of mycelium polysaccharide from liquid fermentation of Monascus purpureus (Hong Qu). Carbohydr Polym. 2021;262:117945. https://doi.org/10.1016/j.carbpol.2021.117945.
21. Cui Y, Zhu L, Li Y, Jiang S, Sun Q, Xie E, Chen H, Zhao Z, Qiao W, Xu J, Dong C. Structure of a laminarin-type β-(1→3)-glucan from brown algae Sargassum

henslowianum and its potential on regulating gut microbiota. Carbohydr Polym. 2021;255:117389. https://doi.org/10.1016/j.carbpol.2020.117389.
22. Xiao M, Jia X, Kang J, Liu Y, Zhang J, Jiang Y, Liu G, Cui SW, Guo Q. Unveiling the breadmaking transformation: Structural and functional insights into Arabinoxylan. Carbohydr Polym. 2024;330:121845. https://doi.org/10.1016/j.carbpol.2024.121845.
23. Kang J, Yue H, Li X, He C, Li Q, Cheng L, Zhang J, Liu Y, Wang S, Guo Q. Structural, rheological and functional properties of ultrasonic treated xanthan gums. Int J Biol Macromol. 2023;246:125650. https://doi.org/10.1016/j.ijbiomac.2023.125650.
24. Wang W, Xu C, Zhou X, Zhang L, Gu L, Liu Z, Ma J, Hou J, Jiang Z. *Lactobacillus plantarum* Combined with Galactooligosaccharides supplement: a neuroprotective regimen against neurodegeneration and memory impairment by regulating short-chain fatty acids and the c-Jun N-terminal kinase signaling pathway in mice. J Agric Food Chem. 2022;70:8619–30. https://doi.org/10.1021/acs.jafc.2c01950.
25. Wan P, Liu H, Ding M, Zhang K, Shang Z, Wang Y, Ma Y. Physicochemical characterization, digestion profile and gut microbiota regulation activity of intracellular polysaccharides from Chlorella zofingiensis. Int J Biol Macromol. 2023;253:126881. https://doi.org/10.1016/j.ijbiomac.2023.126881.
26. Qiao L, Li Y, Chi Y, Ji Y, Gao Y, Hwang H, Aker WG, Wang P. Rheological properties, gelling behavior and texture characteristics of polysaccharide from Enteromorpha prolifera. Carbohydr Polym. 2016;136:1307–14. https://doi.org/10.1016/j.carbpol.2015.10.030.
27. Srishailam K, Balakrishna A, Reddy BV, Rao GR. Insights into structural and vibrational characteristics of 1-methoxy-4-[2-(phenylsulfonyl)vinyl]benzene: An application of experimental vibrational spectroscopy and density functional theory. J Mol Struct. 2023;1286:135572. https://doi.org/10.1016/j.molstruc.2023.135572.
28. Yang F, Nagahawatta DP, Yang H-W, Ryu B, Lee H-G, Je J-G, Heo M-S, Jeon Y-J. In vitro and in vivo immuno-enhancing effect of fucoidan isolated from non-edible brown seaweed Sargassum thunbergii. Int J Biol Macromol. 2023;253:127212. https://doi.org/10.1016/j.ijbiomac.2023.127212.
29. Peng Y, Li Y, Pi Y, Yue X. Effects of almond (Armeniaca Sibirica L. Lam) polysaccharides on gut microbiota and anti-inflammatory effects on LPS-induced RAW264.7 cells. Int J Biol Macromol. 2024;263:130098. https://doi.org/10.1016/j.ijbiomac.2024.130098.
30. Desjardins M, Houde M, Gagnon E. Phagocytosis: the convoluted way from nutrition to adaptive immunity. Immunol Rev. 2005;207:158–65. https://doi.org/10.1111/j.0105-2896.2005.00319.x.
31. Li P, Jing Y, Qiu X, Xiao H, Zheng Y, Wu L. Structural characterization and immunomodulatory activity of a polysaccharide from Dioscotea opposita. Int J Biol Macromol. 2024;265:130734. https://doi.org/10.1016/j.ijbiomac.2024.130734.
32. Chen Y, Zhang H, Wang Y, Nie S, Li C, Xie M. Sulfated modification of the polysaccharides from Ganoderma atrum and their antioxidant and immunomodulating activities. Food Chem. 2015;186:231–8. https://doi.org/10.1016/j.foodchem.2014.10.032.
33. Bi S, Jing Y, Cui X, Gong Y, Zhang J, Feng X, Shi Z, Zheng Q, Li D. A novel polysaccharide isolated from Coriolus versicolor polarizes M2 macrophages into an M1 phenotype and reversesits immunosuppressive effect on tumor microenvironment. Int J Biol Macromol. 2024;259:129352. https://doi.org/10.1016/j.ijbiomac.2024.129352.
34. Taylor ME, Conary JT, Lennartz MR, Stahl PD, Drickamer K. Primary structure of the mannose receptor contains multiple motifs resembling carbohydrate-recognition domains. J Biol Chem. 1990;265:12156–62. https://doi.org/10.1016/S0021-9258(19)38325-5.
35. Ginsburg I. Role of lipoteichoic acid in infection and inflammation. Lancet Infect Dis. 2002;2:171–9. https://doi.org/10.1016/S1473-3099(02)00226-8.
36. Leiro JM, Castro R, Arranz JA, Lamas J. Immunomodulating activities of acidic sulphated polysaccharides obtained from the seaweed Ulva rigida C. Agardh. Int Immunopharmacol. 2007;7:879–88. https://doi.org/10.1016/j.intimp.2007.02.007.
37. Xiao M, Jia X, Wang N, Kang J, Hu X, Goff HD, Cui SW, Ding H, Guo Q. Therapeutic potential of non-starch polysaccharides on type 2 diabetes: from hypoglycemic mechanism to clinical trials. Crit Rev Food Sci Nutr. 2024;64:1177–210. https://doi.org/10.1080/10408398.2022.2113366.
38. Ge Q, Hou C, Rao X, Zhang A, Xiao G, Wang L, Jin K, Sun P, Chen L-C. In vitro fermentation characteristics of polysaccharides from coix seed and its effects on the gut microbiota. Int J Biol Macromol. 2024;262:129994. https://doi.org/10.1016/j.ijbiomac.2024.129994.
39. Wang Z, Zhang X, Zhu L, Yang X, He F, Wang T, Bao T, Lu H, Wang H, Yang S. Inulin alleviates inflammation of alcoholic liver disease via SCFAs-inducing suppression of M1 and facilitation of M2 macrophages in mice. Int Immunopharmacol. 2020;78:106062. https://doi.org/10.1016/j.intimp.2019.106062.
40. Takeuchi T, Miyauchi E, Kanaya T, Kato T, Nakanishi Y, Watanabe T, Kitami T, Taida T, Sasaki T, Negishi H, Shimamoto S, Matsuyama A, Kimura I, Williams IR, Ohara O, Ohno H. Acetate differentially regulates IgA reactivity to commensal bacteria. Nature. 2021;595:560–4. https://doi.org/10.1038/s41586-021-03727-5.
41. Duscha A, Gisevius B, Hirschberg S, Yissachar N, Stangl GI, Dawin E, Bader V, Haase S, Kaisler J, David C, Schneider R, Troisi R, Zent D, Hegelmaier T, Dokalis N, Gerstein S, Del Mare-Roumani S, Amidror S, Staszewski O, Poschmann G, Stühler K, Hirche F, Balogh A, Kempa S, Träger P, Zaiss MM, Holm JB, Massa MG, Nielsen HB, Faissner A, Lukas C, Gatermann SG, Scholz M, Przuntek H, Prinz M, Forslund SK, Winklhofer KF, Müller DN, Linker RA, Gold R, Haghikia A. Propionic acid shapes the multiple sclerosis disease course by an immunomodulatory mechanism. Cell. 2020;180:1067-1080.e16. https://doi.org/10.1016/j.cell.2020.02.035.
42. Ebrahimzadeh Leylabadlo H, Sanaie S, Sadeghpour Heravi F, Ahmadian Z, Ghotaslou R. From role of gut microbiota to microbial-based therapies in type 2-diabetes. Infect Genet Evol. 2020;81:104268. https://doi.org/10.1016/j.meegid.2020.104268.
43. Wang X, Xue J, Zhang R, Li Y, Li X, Ding Y, Feng Y, Zhang X, Yang Y, Su J, Chu X. Prebiotic characteristics of degraded polysaccharides from Acanthopanax senticosus polysaccharide on broilers gut microbiota based on in vitro digestion and fecal fermentation. Poult Sci. 2024;103:103807. https://doi.org/10.1016/j.psj.2024.103807.
44. Wang W, Xu C, Liu Z, Gu L, Ma J, Hou J, Jiang Z. Physicochemical properties and bioactivity of polysaccharides from *Isaria cicadae Miquel* with different extraction processes: effects on gut microbiota and immune response in mice. Food Funct. 2022;13:9268–84. https://doi.org/10.1039/D2FO01646J.
45. Wang N, Zhu F, Chen L, Chen K. Proteomics, metabolomics and metagenomics for type 2 diabetes and its complications. Life Sci. 2018;212:194–202. https://doi.org/10.1016/j.lfs.2018.09.035.
46. Chen W-C, Ko C-H, Su Y-S, Lai W-A, Shen F-T. Metabolic potential and community structure of bacteria in an organic tea plantation. Appl Soil Ecol. 2021;157:103762. https://doi.org/10.1016/j.apsoil.2020.103762.
47. Cao S, Yang L, Xie M, Yu M, Shi T. Peanut-natto improved obesity of high-fat diet mice by regulating gut microbiota and lipid metabolism. J Funct Foods. 2024;112:105956. https://doi.org/10.1016/j.jff.2023.105956.
48. Zhao H, Wang Q, Zhao J, Wang D, Liu H, Gao P, Shen Y, Wu T, Wu X, Zhao Y, Zhang C. Ento-A alleviates DSS-induced experimental colitis in mice by remolding intestinal microbiota to regulate SCFAs metabolism and the Th17 signaling pathway. Biomed Pharmacother. 2024;170:115985. https://doi.org/10.1016/j.biopha.2023.115985.
49. Sun H, Guo Y, Wang H, Yin A, Hu J, Yuan T, Zhou S, Xu W, Wei P, Yin S, Liu P, Guo X, Tang Y, Yan Y, Luo Z, Wang M, Liang Q, Wu P, Zhang A, Zhou Z, Chen Y, Li Y, Li J, Shan J, Zhou W. Gut commensal *Parabacteroides distasonis* alleviates inflammatory arthritis. Gut. 2023;72:1664–77. https://doi.org/10.1136/gutjnl-2022-327756.
50. Zhang J, Liu Y, Wu H, Zhou L. Is Shigella an under-recognized pathogen? A case of pyogenic cervical spondylitis caused by Escherichia coli and Shigella flexneri infection. IDCases. 2024;35:e01930. https://doi.org/10.1016/j.idcr.2024.e01930.
51. Liu J, Wang J, Zhou S, Huang D, Qi G, Chen G. Ginger polysaccharides enhance intestinal immunity by modulating gut microbiota in cyclophosphamide-induced immunosuppressed mice. Int J Biol Macromol. 2022;223:1308–19. https://doi.org/10.1016/j.ijbiomac.2022.11.104.

Publisher's Note